PERGAMON

International Journal of Solids and Structures 39 (2002) 4271–4289

INTERNATIONAL JOURNAL OF SOLIDS and STRUCTURES

www.elsevier.com/locate/ijsolstr

Postbuckling of laminated cylindrical shells with piezoelectric actuators under combined external pressure and heating

Hui-Shen Shen

School of Civil Engineering and Mechanics, Shanghai Jiao Tong University, 1954 Hua Shan Road, Shanghai 200030, China

Received 8 July 2001; received in revised form 20 March 2002

Abstract

A postbuckling analysis is presented for a cross-ply laminated cylindrical shell with piezoelectric actuators subjected to the combined action of external pressure and heating and under electric loading cases. The temperature rise considered is assumed to be a uniform distribution over the shell surface and through the shell thickness and the electric field is assumed to be the transverse component E_Z only. The material properties are assumed to be independent of the temperature and the electric field. The governing equations are based on the classical shell theory with von Kármán–Donnell type of kinematic nonlinearity. The nonlinear prebuckling deformations and initial geometric imperfections of the shell are both taken into account. A boundary layer theory of shell buckling, which includes the effects of nonlinear prebuckling deformations, large deflections in the postbuckling range, and initial geometric imperfections of the shell, is extended to the case of hybrid laminated cylindrical shells. A singular perturbation technique is employed to determine the interactive buckling loads and postbuckling equilibrium paths. The numerical illustrations concern the postbuckling behavior of perfect and imperfect, cross-ply laminated cylindrical thin shells with fully covered or embedded piezoelectric actuators subjected to combined action of external pressure and heating and under different sets of electric loading cases. The effects played by applied voltage, shell geometric parameter, stacking sequence, as well as initial geometric imperfections are studied.

Keywords: Postbuckling; Hybrid laminated cylindrical shell; Thermo-piezoelectric effect; Boundary layer theory of shell buckling; Singular perturbation technique

1. Introduction

The circular cylindrical shell has been used extensively as a structural configuration, mainly in the aerospace industry. One of the recent advances in material and structural engineering is in the field of smart structures which incorporates adaptive materials. By taking advantage of the direct and converse

E-mail address: hsshen@mail.sjtu.edu.cn (H.-S. Shen).

0020-7683/02/$ - see front matter
PII: S0020-7683(02)00262-7

piezoelectric effects, piezoelectric composite structures can combine the traditional performance advantages of composite laminates along with the inherent capability of piezoelectric materials to adapt to their current environment. Therefore, hybrid laminated structures where a substrate made laminated material is coupled with surface bonded or embedded piezoelectric actuator and/or sensor layers are becoming increasingly important.

Numerous studies on the modelling and analysis of hybrid laminated cylindrical shells have been performed (see, for example Tzou and Gadre, 1989; Koconis et al., 1994; Birman and Simonyan, 1994; Tani et al., 1995; Chen et al., 1996; Kapuria et al., 1997; Saravanos, 1997; Correia et al., 1999; Lee and Saravanos, 2000; Balamurugan and Narayanan, 2001). These studies were focused on the cases of linear bending analysis and/or vibration control for which there has been considerable interest in engineering (see Li et al., 2001). Recently, Oh et al. (2000) gave a thermal postbuckling analysis of laminated plates with top and/or bottom surface-bonded actuators subjected to thermal and electric loads. In their analysis nonlinear finite element equations based on layerwise displacement theory were formulated, but their numerical results were only for thin plates and all plates were assumed to have perfect initial configurations. Also recently, Shen (2001) gave a postbuckling analysis of laminated plates with fully covered or embedded piezoelectric actuators subjected to mechanical, thermal and electric loads. In the analysis the transverse shear deformation and initial geometric imperfection of the plate are both accounted for. However, studies on postbuckling of hybrid laminated cylindrical shells containing piezoelectric layers subjected to the combined action of external pressure and heating and under electric loading cases have not been seen in the literature.

It has been shown in Shen and Chen (1988, 1990) that in shell buckling, there is a boundary layer phenomenon where prebuckling and buckling displacement vary rapidly. They suggested a boundary layer theory of shell buckling, which includes the effects of nonlinear prebuckling deformations, large deflections in the postbuckling range, and initial geometric imperfections of the shell. Based on this theory, postbuckling analyses for perfect and imperfect, unstiffened and stiffened, isotropic and multilayered cylindrical shells under various loading cases have been performed by Shen and Chen (1991), Shen et al. (1993), and Shen (1997a–c, 1998a,b, 1999). The present paper extends the previous works to the case of cross-ply laminated cylindrical shells with piezoelectric actuators subjected to the combined action of external pressure and heating and under electric loading cases.

In the present study, the temperature rise considered is assumed to be a uniform distribution over the shell surface and through the shell thickness. The electric field is assumed to be the transverse component E_Z only. Note that temperature can affect the properties of fiber-reinforced composites (see Tsai and Hahn, 1980). In addition, the properties of piezoelectric materials, including piezoelectric constants, vary with temperature. The present analysis does not account for these effects, i.e. it is assumed that temperature variations do not affect material properties. Also the material properties are assumed to be independent of the electric field. The governing equations are based on the classical shell theory with von Kármán–Donnell type of kinematic nonlinearity and including thermo-piezoelectric effects. A singular perturbation technique is employed to determine the interactive buckling loads and postbuckling load–deflection curves. The nonlinear prebuckling deformations and initial geometric imperfections of the shell are both taken into account but, for simplicity, the form of initial geometric imperfection is assumed to be the same as the initial buckling mode of the shell. The numerical illustrations show the full nonlinear postbuckling response of hybrid laminated cylindrical shells containing piezoelectric layers under combined loading conditions.

2. Theoretical development

Consider a circular cylindrical shell with mean radius R, length L, and thickness t, which consists of N plies. Some of the plies can be piezoelectric (see Fig. 1). The shell is referred to a coordinate system (X, Y, Z) in which X and Y are in the axial and circumferential directions of the shell and Z is in the direction of the

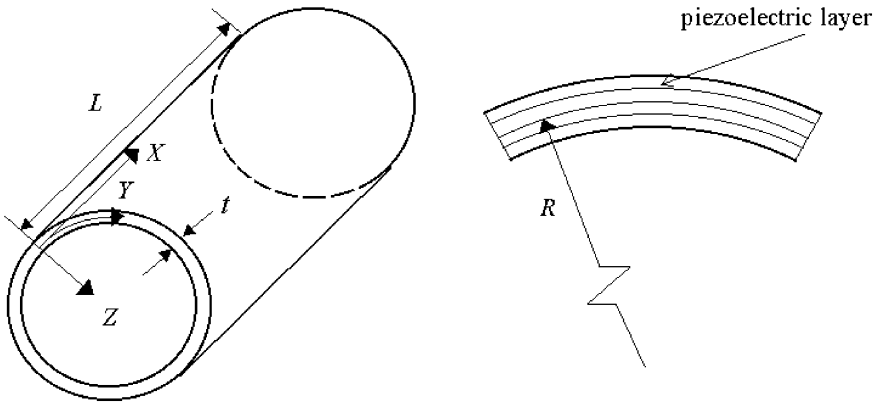

Fig. 1. A hybrid laminated cylindrical shell with piezoelectric layers.

inward normal to the middle surface, the corresponding displacement designated by $\overline{U}$, $\overline{V}$, and $\overline{W}$. The origin of the coordinate system is located at the end of the shell on the middle plane. The shell is assumed to be relatively thin and geometrically imperfect, and is subjected to two loads of external pressure q and a uniform temperature rise T_0 and under electric loading cases. Denoting the initial geometric imperfection by $\overline{W}^*(X,Y)$, let $\overline{W}(X,Y)$ be the additional deflection and $\overline{F}(X,Y)$ be the stress function for the stress resultants defined by $\overline{N}_x = \overline{F}_{,yy}$, $\overline{N}_y = \overline{F}_{,xx}$, and $\overline{N}_{xy} = -\overline{F}_{,xy}$, where a comma denotes partial differentiation with respect to the corresponding coordinates.

It is mentioned that some of the basic equations from Shen (1998b) are repeated here for clarity, with the small changes included that are needed to make them applicable to laminated cylindrical shells with piezoelectric actuators.

Based on classical shell theory (i.e. transverse shear deformation effects are neglected) with von Kármán–Donnell type kinematic relations and including thermo-piezoelectric effects, the governing differential equations for a cross-ply laminated cylindrical shell with fully covered or embedded piezoelectric actuators can be derived in terms of a stress function $\overline{F}$, and a transverse displacement $\overline{W}$, along with the initial geometric imperfection $\overline{W}^*$. They are

$$\widetilde{L}_{11}(\overline{W}) + \widetilde{L}_{12}(\overline{F}) - \widetilde{L}_{13}(\overline{N}^{\mathrm{P}}) - \widetilde{L}_{14}(\overline{M}^{\mathrm{P}}) - \frac{1}{R}\overline{F}_{,xx} = \widetilde{L}(\overline{W} + \overline{W}^*, \overline{F}) + q, \tag{1}$$

$$\widetilde{L}_{21}(\overline{F}) - \widetilde{L}_{22}(\overline{W}) - \widetilde{L}_{23}(\overline{N}^{\mathrm{P}}) + \frac{1}{R}\overline{W}_{,xx} = -\frac{1}{2}\widetilde{L}(\overline{W} + 2\overline{W}^*, \overline{W}), \tag{2}$$

where the operators

$$\begin{aligned}
\widetilde{L}_{13}(\overline{N}^{\mathrm{P}}) &= \frac{\partial^2}{\partial X^2}(B_{11}^*\overline{N}_x^{\mathrm{P}} + B_{21}^*\overline{N}_y^{\mathrm{P}}) + 2\frac{\partial^2}{\partial X \partial Y}(B_{66}^*\overline{N}_{xy}^{\mathrm{P}}) + \frac{\partial^2}{\partial Y^2}(B_{12}^*\overline{N}_x^{\mathrm{P}} + B_{22}^*\overline{N}_y^{\mathrm{P}}),\\
\widetilde{L}_{14}(\overline{M}^{\mathrm{P}}) &= \frac{\partial^2}{\partial X^2}(\overline{M}_x^{\mathrm{P}}) + 2\frac{\partial^2}{\partial X \partial Y}(\overline{M}_{xy}^{\mathrm{P}}) + \frac{\partial^2}{\partial Y^2}(\overline{M}_y^{\mathrm{P}}),\\
\widetilde{L}_{23}(\overline{N}^{\mathrm{P}}) &= \frac{\partial^2}{\partial X^2}(A_{12}^*\overline{N}_x^{\mathrm{P}} + A_{22}^*\overline{N}_y^{\mathrm{P}}) - \frac{\partial^2}{\partial X \partial Y}(A_{66}^*\overline{N}_{xy}^{\mathrm{P}}) + \frac{\partial^2}{\partial Y^2}(A_{11}^*\overline{N}_x^{\mathrm{P}} + A_{12}^*\overline{N}_y^{\mathrm{P}})
\end{aligned} \tag{3}$$

and all other operators are defined as in Shen (1998b).

In Eq. (3), $[A_{ij}^*]$, $[B_{ij}^*]$ and $[D_{ij}^*]$ $(i,j = 1,2,6)$ are reduced stiffness matrices, defined as $\mathbf{A}^* = \mathbf{A}^{-1}$, $\mathbf{B}^* = -\mathbf{A}^{-1}\mathbf{B}$ and $\mathbf{D}^* = \mathbf{D} - \mathbf{B}\mathbf{A}^{-1}\mathbf{B}$, where $\mathbf{A}$, $\mathbf{B}$ and $\mathbf{D}$ are defined in the standard way.

The equivalent thermo-piezoelectric loads are defined as

$$\begin{bmatrix} \overline{N}^{\mathrm{P}} \\ \overline{M}^{\mathrm{P}} \end{bmatrix} = \begin{bmatrix} \overline{N}^{\mathrm{T}} \\ \overline{M}^{\mathrm{T}} \end{bmatrix} + \begin{bmatrix} \overline{N}^{\mathrm{E}} \\ \overline{M}^{\mathrm{E}} \end{bmatrix}. \tag{4}$$

The temperature rise is assumed to be a uniform distribution over the shell surface and through the shell thickness, i.e. $T(X, Y, Z) = T_0$.

For the panel type piezoelectric material, only thickness direction electric field E_Z is dominant, and E_Z is defined as $E_Z = -\Phi_{,Z}$, where Φ is the potential field. If the voltage applied to the actuator in the thickness only, then

$$E_Z = \frac{V_k}{t_k}, \tag{5}$$

where V_k is the applied voltage across the kth ply and t_k is the thickness of the ply.

The forces and moments caused by elevated temperature or electric field are defined by (see Reddy, 1999)

$$\begin{bmatrix} \overline{N}_x^{\mathrm{T}} & \overline{M}_x^{\mathrm{T}} \\ \overline{N}_y^{\mathrm{T}} & \overline{M}_y^{\mathrm{T}} \\ \overline{N}_{xy}^{\mathrm{T}} & \overline{M}_{xy}^{\mathrm{T}} \end{bmatrix} = \sum_{k=1}^{N} \int_{t_{k-1}}^{t_k} (1, Z) \begin{bmatrix} A_x \\ A_y \\ A_{xy} \end{bmatrix}_k T_0 \, \mathrm{d}Z \tag{6a}$$

and

$$\begin{bmatrix} \overline{N}_x^{\mathrm{E}} & \overline{M}_x^{\mathrm{E}} \\ \overline{N}_y^{\mathrm{E}} & \overline{M}_y^{\mathrm{E}} \\ \overline{N}_{xy}^{\mathrm{E}} & \overline{M}_{xy}^{E} \end{bmatrix} = \sum_{k=1}^{N} \int_{t_{k-1}}^{t_k} (1, Z) \begin{bmatrix} B_x \\ B_y \\ B_{xy} \end{bmatrix}_k \frac{V_k}{t_k} \, \mathrm{d}Z \tag{6b}$$

in which

$$\begin{bmatrix} A_x \\ A_y \\ A_{xy} \end{bmatrix} = - \begin{bmatrix} \overline{Q}_{11} & \overline{Q}_{12} & \overline{Q}_{16} \\ \overline{Q}_{12} & \overline{Q}_{22} & \overline{Q}_{26} \\ \overline{Q}_{16} & \overline{Q}_{26} & \overline{Q}_{66} \end{bmatrix} \begin{bmatrix} c^2 & s^2 \\ s^2 & c^2 \\ 2cs & -2cs \end{bmatrix} \begin{bmatrix} \alpha_{11} \\ \alpha_{22} \end{bmatrix}, \tag{7a}$$

$$\begin{bmatrix} B_x \\ B_y \\ B_{xy} \end{bmatrix} = - \begin{bmatrix} \overline{Q}_{11} & \overline{Q}_{12} & \overline{Q}_{16} \\ \overline{Q}_{12} & \overline{Q}_{22} & \overline{Q}_{26} \\ \overline{Q}_{16} & \overline{Q}_{26} & \overline{Q}_{66} \end{bmatrix} \begin{bmatrix} c^2 & s^2 \\ s^2 & c^2 \\ 2cs & -2cs \end{bmatrix} \begin{bmatrix} d_{31} \\ d_{32} \end{bmatrix}, \tag{7b}$$

where α_{11} and α_{22} are the thermal expansion coefficients measured in the fiber and transverse directions, respectively, d_{31} and d_{32} are piezoelectric strain constants of a single ply, and $\overline{Q}_{ij}$ are the transformed elastic constants, details of which can be found in Shen (1997c), and $c = \cos\theta$, $s = \sin\theta$, where θ is the lamination angle with respect to the shell X-axis.

The two end edges of the shell are assumed to be simply supported or clamped, and restrained against expansion longitudinally while the temperature is increased steadily, so that the boundary conditions are

$X = 0, L$:

$$\overline{W} = 0, \tag{8a}$$

$$\overline{U} = 0, \tag{8b}$$

$$\overline{M}_x = -B_{21}^* \frac{\partial^2 \overline{F}}{\partial X^2} - B_{11}^* \frac{\partial^2 \overline{F}}{\partial Y^2} - D_{11}^* \frac{\partial^2 \overline{W}}{\partial X^2} - D_{12}^* \frac{\partial^2 \overline{W}}{\partial Y^2} + \overline{M}_x^{\mathrm{P}} = 0 \quad \text{(simply supported)}, \tag{8c}$$

$$\overline{W}_{,x} = 0 \quad \text{(clamped)}, \tag{8d}$$

where $\overline{M}_x$ is the bending moment. Also, we have the closed (or periodicity) condition

$$\int_0^{2\pi R} \frac{\partial \overline{V}}{\partial Y}\,\mathrm{d}Y = 0 \tag{9a}$$

or

$$\int_0^{2\pi R}\left[A_{22}^*\frac{\partial^2\overline{F}}{\partial X^2}+A_{12}^*\frac{\partial^2\overline{F}}{\partial Y^2}-\left(B_{21}^*\frac{\partial^2\overline{W}}{\partial X^2}+B_{22}^*\frac{\partial^2\overline{W}}{\partial Y^2}\right)+\frac{\overline{W}}{R}-\frac{1}{2}\left(\frac{\partial\overline{W}}{\partial Y}\right)^2-\frac{\partial\overline{W}}{\partial Y}\frac{\partial\overline{W}^*}{\partial Y}-\left(A_{12}^*\overline{N}_x^{\mathrm{P}}+A_{22}^*\overline{N}_y^{\mathrm{P}}\right)\right]\mathrm{d}Y=0. \tag{9b}$$

Because of Eqs. (9a) and (9b), the in-plane boundary condition $\overline{V} = 0$ (at $X = 0, L$) is not needed in Eqs. (8a)–(8d).

The average end-shortening relationship is defined as

$$\begin{aligned}\frac{\Delta_x}{L} &= -\frac{1}{2\pi RL}\int_0^{2\pi R}\int_0^L \frac{\partial\overline{U}}{\partial X}\,\mathrm{d}X\,\mathrm{d}Y\\ &= -\frac{1}{2\pi RL}\int_0^{2\pi R}\int_0^L\left[A_{11}^*\frac{\partial^2\overline{F}}{\partial Y^2}+A_{12}^*\frac{\partial^2\overline{F}}{\partial X^2}-\left(B_{11}^*\frac{\partial^2\overline{W}}{\partial X^2}+B_{12}^*\frac{\partial^2\overline{W}}{\partial Y^2}\right)-\frac{1}{2}\left(\frac{\partial\overline{W}}{\partial X}\right)^2-\frac{\partial\overline{W}}{\partial X}\frac{\partial\overline{W}^*}{\partial X}\right.\\ &\quad\left.-\left(A_{11}^*\overline{N}_x^{\mathrm{P}}+A_{12}^*\overline{N}_y^{\mathrm{P}}\right)\right]\mathrm{d}X\,\mathrm{d}Y.\end{aligned} \tag{10}$$

It is noted that the thermo-piezoelectric forces $\overline{N}_x^{\mathrm{P}}$ and $\overline{N}_y^{\mathrm{P}}$, and moment $\overline{M}_x^{\mathrm{P}}$ are now included in Eqs. (8c), (9b) and (10).

3. Analytical method and asymptotic solutions

Having developed the theory, we will try to solve Eqs. (1) and (2) with boundary condition (8a)–(8d). Before proceeding, it is convenient first to define the following dimensionless quantities:

$$\begin{aligned}&x=\pi X/L,\quad y=Y/R,\quad \beta=L/\pi R,\quad \overline{Z}=L^2/Rt,\quad \varepsilon=(\pi^2R/L^2)[D_{11}^*D_{22}^*A_{11}^*A_{22}^*]^{1/4},\\ &(W,W^*)=\varepsilon(\overline{W},\overline{W}^*)/[D_{11}^*D_{22}^*A_{11}^*A_{22}^*]^{1/4},\quad F=\varepsilon^2\overline{F}/[D_{11}^*D_{22}^*]^{1/2},\\ &\gamma_{12}=(D_{12}^*+2D_{66}^*)/D_{11}^*,\quad \gamma_{22}=(A_{12}^*+\tfrac{1}{2}A_{66}^*)/A_{22}^*,\\ &\gamma_{14}=[D_{22}^*/D_{11}^*]^{1/2},\quad \gamma_{24}=[A_{11}^*/A_{22}^*]^{1/2},\quad \gamma_5=-A_{12}^*/A_{22}^*,\\ &(\gamma_{30},\gamma_{32},\gamma_{34},\gamma_{311},\gamma_{322})=(B_{21}^*,B_{11}^*+B_{22}^*-2B_{66}^*,B_{12}^*,B_{11}^*,B_{22}^*)/[D_{11}^*D_{22}^*A_{11}^*A_{22}^*]^{1/4},\\ &(\gamma_{T1},\gamma_{T2},\gamma_{P1},\gamma_{P2})=(A_x^{\mathrm{T}}/\alpha_0,A_y^{\mathrm{T}}/\alpha_0,B_x^{\mathrm{P}},B_y^{\mathrm{P}})R[A_{11}^*A_{22}^*/D_{11}^*D_{22}^*]^{1/4},\\ &(M_x,M_x^{\mathrm{P}})=\varepsilon^2(\overline{M}_x,\overline{M}_x^{\mathrm{P}})(L^2/\pi^2)/D_{11}^*[D_{11}^*D_{22}^*A_{11}^*A_{22}^*]^{1/4},\\ &\lambda_T=\alpha_0T_0,\quad \lambda_q=q(3)^{3/4}LR^{3/2}[A_{11}^*A_{22}^*]^{1/8}/4\pi[D_{11}^*D_{22}^*]^{3/8},\\ &\delta_T=(\Delta_x/L)/(2/R)[D_{11}^*D_{22}^*A_{11}^*A_{22}^*]^{1/4},\quad \delta_q=(\Delta_x/L)(3)^{3/4}LR^{1/2}/4\pi[D_{11}^*D_{22}^*A_{11}^*A_{22}^*]^{3/8},\end{aligned} \tag{11}$$

where α_0 is an arbitrary reference value, and

$$\alpha_{11}=a_{11}\alpha_0,\qquad \alpha_{22}=a_{22}\alpha_0. \tag{12}$$

Also let

$$\begin{bmatrix} A_x^{\mathrm{T}} \\ A_y^{\mathrm{T}} \end{bmatrix} = -\sum_{k=1}^{N} \int_{t_{k-1}}^{t_k} \begin{bmatrix} A_x \\ A_y \end{bmatrix}_k \mathrm{d}Z, \tag{13a}$$

$$\begin{bmatrix} B_x^{\mathrm{P}} \\ B_y^{\mathrm{P}} \end{bmatrix} \Delta V = -\sum_{k=1}^{N} \int_{t_{k-1}}^{t_k} \begin{bmatrix} B_x \\ B_y \end{bmatrix}_k \frac{V_k}{t_k} \mathrm{d}Z. \tag{13b}$$

The nonlinear Eqs. (1) and (2) may then be written in dimensionless form as

$$\varepsilon^2 L_{11}(W) + \varepsilon\gamma_{14} L_{12}(F) - \gamma_{14} F_{,xx} = \gamma_{14}\beta^2 L(W + W^*, F) + \gamma_{14}\tfrac{4}{3}(3)^{1/4}\lambda_q \varepsilon^{3/2}, \tag{14}$$

$$L_{21}(F) - \varepsilon\gamma_{24} L_{22}(W) + \gamma_{24} W_{,xx} = -\tfrac{1}{2}\gamma_{24}\beta^2 L(W + 2W^*, W), \tag{15}$$

where the operators can also be found in Shen (1998b).

Because of the definition of ε given in Eq. (11), for most of the composite materials $[D_{11}^* D_{22}^* A_{11}^* A_{22}^*]^{1/4} = (0.2 - 0.3)t$, hence when $\overline{Z} = (L^2/Rt) > 2.96$, we have $\varepsilon < 1$. In particular, for isotropic cylindrical shells, we have $\varepsilon = \pi^2/\overline{Z}_{\mathrm{B}}\sqrt{12}$, where $\overline{Z}_{\mathrm{B}} = (L^2/Rt)[1 - \nu^2]^{1/2}$ is the Batdorf shell parameter, which should be greater than 2.85 in the case of classical linear buckling analysis (see Batdorf, 1947). In practice, the shell structure will have $\overline{Z} \geqslant 10$, so that we always have $\varepsilon \ll 1$. When $\varepsilon < 1$, Eqs. (14) and (15) are equations of the boundary layer type, from which nonlinear prebuckling deformations, large deflections in the postbuckling range, and initial geometric imperfections of the shell can be considered simultaneously.

The boundary conditions expressed by Eqs. (8a)–(8d) become

$x = 0,\ \pi$:

$$W = 0, \tag{16a}$$

$$\delta_q \text{ (or } \delta_T) = 0, \tag{16b}$$

$$M_x = 0 \quad \text{(simply supported)}, \tag{16c}$$

$$W_{,x} = 0 \quad \text{(clamped)} \tag{16d}$$

and the closed condition becomes

$$\int_0^{2\pi} \left[\left(\frac{\partial^2 F}{\partial x^2} - \gamma_5 \beta^2 \frac{\partial^2 F}{\partial y^2} \right) - \varepsilon\gamma_{24} \left(\gamma_{30} \frac{\partial^2 W}{\partial x^2} + \gamma_{322}\beta^2 \frac{\partial^2 W}{\partial y^2} \right) + \gamma_{24} W - \frac{1}{2}\gamma_{24}\beta^2 \left(\frac{\partial W}{\partial y} \right)^2 \right.$$
$$\left. - \gamma_{24}\beta^2 \frac{\partial W}{\partial y} \frac{\partial W^*}{\partial y} + \varepsilon(\gamma_{T2} - \gamma_5\gamma_{T1})\lambda_T + \varepsilon(\gamma_{p2} - \gamma_5\gamma_{p1})\Delta V \right] \mathrm{d}y = 0. \tag{17}$$

In this section two combined loading conditions will be considered, so that the unit end-shortening relationship may be written in two dimensionless forms as

$$\delta_q = -\frac{(3)^{3/4}}{8\pi^2\gamma_{24}} \varepsilon^{-3/2} \int_0^{2\pi} \int_0^{\pi} \left[\left(\gamma_{24}^2 \beta^2 \frac{\partial^2 F}{\partial y^2} - \gamma_5 \frac{\partial^2 F}{\partial x^2} \right) - \varepsilon\gamma_{24} \left(\gamma_{311} \frac{\partial^2 W}{\partial x^2} + \gamma_{34}\beta^2 \frac{\partial^2 W}{\partial y^2} \right) \right.$$
$$\left. - \frac{1}{2}\gamma_{24} \left(\frac{\partial W}{\partial x} \right)^2 - \gamma_{24} \frac{\partial W}{\partial x} \frac{\partial W^*}{\partial x} + \varepsilon(\gamma_{24}^2\gamma_{T1} - \gamma_5\gamma_{T2})\lambda_T + \varepsilon(\gamma_{24}^2\gamma_{P1} - \gamma_5\gamma_{P2})\Delta V \right] \mathrm{d}x\,\mathrm{d}y, \tag{18a}$$

$$\delta_T = -\frac{1}{4\pi^2\gamma_{24}}\varepsilon^{-1}\int_0^{2\pi}\int_0^{\pi}\left[\left(\gamma_{24}^2\beta^2\frac{\partial^2 F}{\partial y^2}-\gamma_5\frac{\partial^2 F}{\partial x^2}\right)-\varepsilon\gamma_{24}\left(\gamma_{311}\frac{\partial^2 W}{\partial x^2}+\gamma_{34}\beta^2\frac{\partial^2 W}{\partial y^2}\right)\right.$$
$$\left.-\frac{1}{2}\gamma_{24}\left(\frac{\partial W}{\partial x}\right)^2-\gamma_{24}\frac{\partial W}{\partial x}\frac{\partial W^*}{\partial x}+\varepsilon(\gamma_{24}^2\gamma_{T1}-\gamma_5\gamma_{T2})\lambda_T+\varepsilon(\gamma_{24}^2\gamma_{P1}-\gamma_5\gamma_{P2})\Delta V\right]\mathrm{d}x\,\mathrm{d}y. \tag{18b}$$

By virtue of the fact that ΔV and T_0 are assumed to be uniform, the thermo-piezoelectric coupling in Eqs. (1) and (2) vanishes, but terms in ΔV and λ_T intervene in Eqs. (17)–(18b).

Applying Eqs. (14)–(18b), the postbuckling behavior of perfect and imperfect, cross-ply laminated cylindrical shells with piezoelectric actuators under combined loading conditions is determined by a singular perturbation technique. The essence of this procedure, in the present case, is to assume that

$$\begin{aligned} W &= w(x,y,\varepsilon)+\widetilde{W}(x,\xi,y,\varepsilon)+\widehat{W}(x,\varsigma,y,\varepsilon),\\ F &= f(x,y,\varepsilon)+\widetilde{F}(x,\xi,y,\varepsilon)+\widehat{F}(x,\varsigma,y,\varepsilon), \end{aligned} \tag{19}$$

where ε is a small perturbation parameter (see beneath Eq. (15)) and $w(x,y,\varepsilon)$, $f(x,y,\varepsilon)$ are called outer solutions or regular solutions of the shell, $\widetilde{W}(x,\xi,y,\varepsilon)$, $\widetilde{F}(x,\xi,y,\varepsilon)$ and $\widehat{W}(x,\varsigma,y,\varepsilon)$, $\widehat{F}(x,\varsigma,y,\varepsilon)$ are the boundary layer solutions near the $x=0$ and $x=\pi$ edges, respectively, and ξ and ζ are the boundary layer variables, defined as

$$\xi = x/\sqrt{\varepsilon}, \qquad \varsigma = (\pi-x)/\sqrt{\varepsilon}. \tag{20}$$

(This means for isotropic cylindrical shells that the width of the boundary layers is of order $\sqrt{Rt}$.) In Eq. (19) the regular and boundary layer solutions are taken in the forms of perturbation expansions as

$$w(x,y,\varepsilon)=\sum_{j=1}\varepsilon^{j/2}w_{j/2}(x,y), \qquad f(x,y,\varepsilon)=\sum_{j=0}\varepsilon^{j/2}f_{j/2}(x,y), \tag{21a}$$

$$\widetilde{W}(x,\xi,y,\varepsilon)=\sum_{j=0}\varepsilon^{j/2+1}\widetilde{W}_{j/2+1}(x,\xi,y), \qquad \widetilde{F}(x,\xi,y,\varepsilon)=\sum_{j=0}\varepsilon^{j/2+2}\widetilde{F}_{j/2+2}(x,\xi,y), \tag{21b}$$

$$\widehat{W}(x,\varsigma,y,\varepsilon)=\sum_{j=0}\varepsilon^{j/2+1}\widehat{W}_{j/2+1}(x,\varsigma,y), \qquad \widehat{F}(x,\varsigma,y,\varepsilon)=\sum_{j=0}\varepsilon^{j/2+2}\widehat{F}_{j/2+2}(x,\varsigma,y). \tag{21c}$$

The initial buckling mode is assumed to have the form

$$w_2(x,y)=A_{11}^{(2)}\sin mx\sin ny \tag{22}$$

and the initial geometric imperfection is assumed to have the similar form

$$W^*(x,y,\varepsilon)=\varepsilon^2 a_{11}^*\sin mx\sin ny=\varepsilon^2\mu A_{11}^{(2)}\sin mx\sin ny, \tag{23}$$

where $\mu=a_{11}^*/A_{11}^{(2)}$ is the imperfection parameter.

Substituting Eqs. (19)–(21c) into Eqs. (14) and (15), and collecting terms of the same order of ε, three sets of perturbation equations are obtained for the regular and boundary layer solutions, respectively. It has been shown (Shen and Chen, 1988; Shen, 1997b) that the effect of the boundary layer on the buckling load of the shell under thermal loading is quite different from that of the shell subjected to external pressure. To this end, two kinds of combined loading conditions will be considered.

Case (1): High values of external pressure combined with relatively low thermal load. Let

$$\frac{2\lambda_C\varepsilon}{\frac{4}{3}(3)^{1/4}\lambda_q\varepsilon^{3/2}}=\frac{b_1}{2}, \tag{24}$$

where $\lambda_C = \sigma_x(Rt/2)\,[A_{11}^* A_{22}^*/D_{11}^* D_{22}^*]^{1/4}$, σ_x is the average axial compressive stress caused by temperature rise T_0, so that $\lambda_C = (\gamma_{24}^2\gamma_{T1} - \gamma_5\gamma_{T2})\lambda_T/2\gamma_{24}^2$. (This means for isotropic cylindrical shells $\sigma_x = E\alpha T_0$, and it is a well-known result.)

By taking $a_1 = a + b_1$, where $a = 2\gamma_5/\gamma_{24}^2$, and by using Eqs. (22) and (23) to solve these perturbation equations of each order, and matching the regular solutions with the boundary layer solutions at each end of the shell, so that the asymptotic solutions satisfying the clamped boundary conditions are constructed as

$$\begin{aligned} W = {} & \varepsilon^{3/2}\left[A_{00}^{(3/2)} - A_{00}^{(3/2)}\left(\cos\phi\frac{x}{\sqrt{\varepsilon}} + \frac{\alpha}{\phi}\sin\phi\frac{x}{\sqrt{\varepsilon}}\right)\exp\left(-\alpha\frac{x}{\sqrt{\varepsilon}}\right)\right. \\ & \left. - A_{00}^{(3/2)}\left(\cos\phi\frac{\pi-x}{\sqrt{\varepsilon}} + \frac{\alpha}{\phi}\sin\phi\frac{\pi-x}{\sqrt{\varepsilon}}\right)\exp\left(-\alpha\frac{\pi-x}{\sqrt{\varepsilon}}\right)\right] + \varepsilon^2[A_{11}^{(2)}\sin mx\sin ny] \\ & + \varepsilon^3[A_{11}^{(3)}\sin mx\sin ny] + \varepsilon^4[A_{00}^{(4)} + A_{20}^{(4)}\sin 2mx + A_{02}^{(4)}\cos 2ny] + \mathrm{O}(\varepsilon^5), \end{aligned} \tag{25}$$

$$\begin{aligned} F = {} & -\frac{1}{2}B_{00}^{(0)}\left(\beta^2x^2 + a_1\frac{y^2}{2}\right) + \varepsilon\left[-\frac{1}{2}B_{00}^{(1)}\left(\beta^2x^2 + a_1\frac{y^2}{2}\right)\right] + \varepsilon^2\left[-\frac{1}{2}B_{00}^{(2)}\left(\beta^2x^2 + a_1\frac{y^2}{2}\right)\right. \\ & \left. + B_{11}^{(2)}\sin mx\sin ny\right] + \varepsilon^{5/2}\left[A_{00}^{(3/2)}\left(\gamma_{24}\left(\frac{1}{b}+\gamma_{30}\right)\cos\phi\frac{x}{\sqrt{\varepsilon}} - \gamma_{24}\left(\frac{1}{b}-\gamma_{30}\right)\frac{\alpha}{\phi}\sin\phi\frac{x}{\sqrt{\varepsilon}}\right)\right. \\ & \times\exp\left(-\alpha\frac{x}{\sqrt{\varepsilon}}\right) + A_{00}^{(3/2)}\left(\gamma_{24}\left(\frac{1}{b}+\gamma_{30}\right)\cos\phi\frac{\pi-x}{\sqrt{\varepsilon}} - \gamma_{24}\left(\frac{1}{b}-\gamma_{30}\right)\frac{\alpha}{\phi}\sin\phi\frac{\pi-x}{\sqrt{\varepsilon}}\right) \\ & \left.\times\exp\left(-\alpha\frac{\pi-x}{\sqrt{\varepsilon}}\right)\right] + \varepsilon^3\left[-\frac{1}{2}B_{00}^{(3)}\left(\beta^2x^2 + a_1\frac{y^2}{2}\right)\right] + \varepsilon^4\left[-\frac{1}{2}B_{00}^{(4)}\left(\beta^2x^2 + a_1\frac{y^2}{2}\right)\right. \\ & \left. + B_{11}^{(4)}\sin mx\sin ny + B_{20}^{(4)}\cos 2mx + B_{02}^{(4)}\cos 2ny\right] + \mathrm{O}(\varepsilon^5). \end{aligned} \tag{26}$$

Note that all coefficients in Eqs. (25) and (26) are related and can be written as functions of $A_{11}^{(2)}$, but for the sake of brevity the detailed expressions are not shown, whereas α and ϕ are given in detail in Appendix A.

Next, upon substitution of Eqs. (25) and (26) into the boundary condition $\delta_q = 0$, the postbuckling equilibrium path can be written as

$$\lambda_q = \frac{1}{4}(3)^{3/4}\varepsilon^{-3/2}[\lambda_q^{(0)} + \lambda_q^{(2)}(A_{11}^{(2)}\varepsilon^2)^2 + \cdots]. \tag{27}$$

In Eq. (27), $(A_{11}^{(2)}\varepsilon^2)$ is taken as the second perturbation parameter relating to the dimensionless maximum deflection. If the maximum deflection is assumed to be at the point $(x, y) = (\pi/2m, \pi/2n)$, from Eq. (25) one has

$$A_{11}^{(2)}\varepsilon^2 = W_{\mathrm{m}} - \Theta_1 W_{\mathrm{m}}^2 + \cdots, \tag{28a}$$

where W_{m} is the dimensionless form of maximum deflection of the shell that can be written as

$$W_{\mathrm{m}} = \frac{1}{C_3}\left[\varepsilon\frac{t}{[D_{11}^* D_{22}^* A_{11}^* A_{22}^*]^{1/4}}\frac{\overline{W}}{t} + \Theta_2\right]. \tag{28b}$$

All symbols used in Eqs. (27)–(28b) and Eqs. (32)–(33b) below are also described in detail in Appendix A.

Case (2): High values of temperature rise combined with relatively low external pressure. Let

$$\frac{\frac{4}{3}(3)^{1/4}\lambda_q\varepsilon^{3/2}}{2\lambda_C\varepsilon} = 2b_2. \tag{29}$$

Similarly, by taking $a_2 = 2b_2$ and using a singular perturbation procedure, the asymptotic solutions satisfying the clamped boundary conditions are obtained as

$$\begin{aligned} W = \varepsilon\Bigg[& A_{00}^{(1)} - A_{00}^{(1)}\left(\cos\phi\frac{x}{\sqrt{\varepsilon}} + \frac{\alpha}{\phi}\sin\phi\frac{x}{\sqrt{\varepsilon}}\right)\exp\left(-\alpha\frac{x}{\sqrt{\varepsilon}}\right) - A_{00}^{(1)}\left(\cos\phi\frac{\pi-x}{\sqrt{\varepsilon}} + \frac{\alpha}{\phi}\sin\phi\frac{\pi-x}{\sqrt{\varepsilon}}\right) \\ & \times\exp\left(-\alpha\frac{\pi-x}{\sqrt{\varepsilon}}\right)\Bigg] + \varepsilon^2\Bigg[A_{11}^{(2)}\sin mx\sin ny + A_{02}^{(2)}\cos 2ny - A_{02}^{(2)}\cos 2ny \\ & \times\left(\cos\phi\frac{x}{\sqrt{\varepsilon}} + \frac{\alpha}{\phi}\sin\phi\frac{x}{\sqrt{\varepsilon}}\right)\exp\left(-\alpha\frac{x}{\sqrt{\varepsilon}}\right) - A_{02}^{(2)}\cos 2ny\left(\cos\phi\frac{\pi-x}{\sqrt{\varepsilon}} + \frac{\alpha}{\phi}\sin\phi\frac{\pi-x}{\sqrt{\varepsilon}}\right) \\ & \times\exp\left(-\alpha\frac{\pi-x}{\sqrt{\varepsilon}}\right)\Bigg] + \varepsilon^3[A_{11}^{(3)}\sin mx\sin ny + A_{02}^{(3)}\cos 2ny] + \varepsilon^4[A_{00}^{(4)} + A_{20}^{(4)}\sin 2mx \\ & + A_{02}^{(4)}\cos 2ny + A_{13}^{(4)}\sin mx\sin 3ny + A_{04}^{(4)}\cos 4ny] + \mathrm{O}(\varepsilon^5), \end{aligned} \tag{30}$$

$$\begin{aligned} F = & -\frac{1}{2}B_{00}^{(0)}(y^2 + a_2\beta^2x^2) + \varepsilon\left[-\frac{1}{2}B_{00}^{(1)}(y^2 + a_2\beta^2x^2)\right] + \varepsilon^2\Bigg[-\frac{1}{2}B_{00}^{(2)}(y^2 + a_2\beta^2x^2) + B_{11}^{(2)}\sin mx\sin ny \\ & + A_{00}^{(1)}\left(\gamma_{24}\left(\frac{1}{b} + \gamma_{30}\right)\cos\phi\frac{x}{\sqrt{\varepsilon}} - \gamma_{24}\left(\frac{1}{b} - \gamma_{30}\right)\frac{\alpha}{\phi}\sin\phi\frac{x}{\sqrt{\varepsilon}}\right)\exp\left(-\alpha\frac{x}{\sqrt{\varepsilon}}\right) \\ & + A_{00}^{(1)}\left(\gamma_{24}\left(\frac{1}{b} + \gamma_{30}\right)\cos\phi\frac{\pi-x}{\sqrt{\varepsilon}} - \gamma_{24}\left(\frac{1}{b} - \gamma_{30}\right)\frac{\alpha}{\phi}\sin\phi\frac{\pi-x}{\sqrt{\varepsilon}}\right)\exp\left(-\alpha\frac{\pi-x}{\sqrt{\varepsilon}}\right)\Bigg] \\ & + \varepsilon^3\Bigg[-\frac{1}{2}B_{00}^{(3)}(y^2 + a_2\beta^2x^2) + B_{02}^{(3)}\cos 2ny + A_{02}^{(2)}\cos 2ny\left(\gamma_{24}\left(\frac{1}{b} + \gamma_{30}\right)\cos\phi\frac{x}{\sqrt{\varepsilon}}\right. \\ & \left. - \gamma_{24}\left(\frac{1}{b} - \gamma_{30}\right)\frac{\alpha}{\phi}\sin\phi\frac{x}{\sqrt{\varepsilon}}\right)\exp\left(-\alpha\frac{x}{\sqrt{\varepsilon}}\right) + A_{02}^{(2)}\cos 2ny\left(\gamma_{24}\left(\frac{1}{b} + \gamma_{30}\right)\cos\phi\frac{\pi-x}{\sqrt{\varepsilon}}\right. \\ & \left. - \gamma_{24}\left(\frac{1}{b} - \gamma_{30}\right)\frac{\alpha}{\phi}\sin\phi\frac{\pi-x}{\sqrt{\varepsilon}}\right)\exp\left(-\alpha\frac{\pi-x}{\sqrt{\varepsilon}}\right)\Bigg] + \varepsilon^4\Bigg[-\frac{1}{2}B_{00}^{(4)}(y^2 + a_2\beta^2x^2) \\ & + B_{11}^{(4)}\sin mx\sin ny + B_{20}^{(4)}\cos 2mx + B_{02}^{(4)}\cos 2ny + B_{13}^{(4)}\sin mx\sin 3ny\Bigg] + \mathrm{O}(\varepsilon^5). \end{aligned} \tag{31}$$

Next, upon substitution of Eqs. (30) and (31) into the boundary condition $\delta_T = 0$, the thermal postbuckling equilibrium path can be written as

$$\lambda_T = \lambda_T^{(0)} - \lambda_T^{(P)} - \lambda_T^{(2)}(A_{11}^{(2)}\varepsilon)^2 + \lambda_T^{(4)}(A_{11}^{(2)}\varepsilon)^4 + \cdots \tag{32}$$

In Eq. (32), similarly, $(A_{11}^{(2)}\varepsilon)$ is taken as the second perturbation parameter in this case, and we have

$$A_{11}^{(2)}\varepsilon = W_{\mathrm{m}} - \Theta_3 W_{\mathrm{m}}^2 + \cdots \tag{33a}$$

and the dimensionless maximum deflection of the shell is written as

$$W_{\mathrm{m}} = \frac{1}{C_3}\left[\frac{t}{[D_{11}^* D_{22}^* A_{11}^* A_{22}^*]^{1/4}}\frac{\overline{W}}{t} + \Theta_4\right]. \tag{33b}$$

Eqs. (27)–(28b) and (32)–(33b) can be employed to obtain numerical results for full nonlinear postbuckling load–deflection curves of cross-ply laminated cylindrical shells with piezoelectric actuators subjected to combined action of external pressure and heating and under electric loading cases. Buckling under a uniform lateral pressure and thermal buckling under a uniform temperature rise follow as two limiting cases. By increasing b_1 and b_2, respectively, the interaction curve of a hybrid laminated cylindrical shell under combined loading can be constructed with these two lines. Note that since $b_2 = 1/b_1$, only one

load-proportional parameter should be determined in advance. The initial buckling load of a perfect shell can readily be obtained numerically, by setting $\overline{W}^*/t = 0$ (or $\mu = 0$), while taking $\overline{W}/t = 0$ (note that $W_m \neq 0$). In this case, the minimum buckling load is determined by considering Eq. (27) or (32) for various values of the buckling mode (m, n) that determine the number of half-waves in the X-direction and of full waves in the Y-direction. Note that because of Eqs. (25) and (30), the prebuckling deformation of the shell is nonlinear.

4. Numerical results and comments

Numerical results are presented in this section for perfect and imperfect, cross-ply laminated cylindrical shells with symmetrically fully covered or embedded piezoelectric layers, where the outmost layer is the first mentioned orientation. Graphite/epoxy composite material and PZT-5A were selected for the substrate orthotropic layers and piezoelectric layers, respectively. The material properties of the graphite/epoxy and piezoelectric layers are given in Table 1. However, the analysis is equally applicable to other types of composite materials. For these examples, the total thickness of the shell $t = 1.2$ mm whereas the thickness of piezoelectric layers is 0.1 mm, and all other orthotropic layers are of equal thickness.

The accuracy and effectiveness of the present method for the buckling and postbuckling analysis of isotropic or multilayered cylindrical shells subjected to external pressure or thermal loading were examined by many comparison studies given in Shen and Chen (1991), Shen et al. (1993), and Shen (1998a,b).

A parametric study has been carried out and typical results are shown in Tables 2 and 3, and Figs. 2–8. It should be appreciated that in all of these figures $\overline{W}^*/t$ denotes the dimensionless maximum initial geometric imperfection of the shell.

Table 2 gives buckling loads T_{cr}, (°C) and q_{cr} (kPa) for $(0/90)_{2S}$ symmetric cross-ply and $(0/90)_{4T}$ anti-symmetric cross-ply laminated cylindrical shells with symmetrically fully covered or embedded piezoelectric layers, referred to as $(P/(0/90)_2)_S$, $(0/P/90/0/90)_S$, $(P/(0/90)_4/P)_T$ and $(0/P/(90/0)_3/P/90)_T$, respectively, under four sets of combined loading conditions, i.e. lateral pressure alone ($b_1 = 0$), combined loading case (1) ($b_1 = 10$), combined loading case (2) ($b_2 = 0.01$ or 0.02) and heating alone ($b_2 = 0$). The control voltage with the same sign is also applied to both upper and lower piezoelectric layer, referred to as V_U and V_L. Three electric loading cases are considered. Here, $V_U = V_L = 0$ V means the buckling under a grounding condition. It can be seen that the control voltage has a significant effect on the buckling loads under combined loading case (2), but has a very small effect on the buckling loads under combined loading case (1).

Fig. 2 gives the thermal postbuckling load–deflection curves for a $(P/(0/90)_2)_S$ cylindrical shell under combined loading case (2) with the load-proportional parameter $b_2 = 0$ and 0.02, and under three sets of

Table 1
Material properties of the graphite/epoxy and PZT-5A layers used in the present study

Properties	Graphite/epoxy	PZT-5A layer
E_{11} (GPa)	150	63
E_{22} (GPa)	9	63
G_{12} (GPa)	7.1	24.2
ν_{12}	0.3	0.3
α_{11} (10^{-6} °C^{-1})	1.1	0.9
α_{22} (10^{-6} °C^{-1})	25.2	0.9
d_{31} (10^{-12} m/V)	0	254
d_{32} (10^{-12} m/V)	0	254

Table 2
Comparisons of buckling loads T_{cr} (°C) and q_{cr} (kPa) for perfect piezolaminated cylindrical shells ($R/t = 300$) subjected to combined heating and lateral pressure and under three sets of electric loading cases

Lay-up	Loading case[a]	$V_U = V_L = -100$ V		$V_U = V_L = 0$ V		$V_U = V_L = +100$ V	
		T_{cr}	q_{cr}	T_{cr}	q_{cr}	T_{cr}	q_{cr}
$\overline{Z} = 200$							
$(P/(0/90)_2)_S$	I	428.7977	0	409.5240	0	390.2303	0
	II	407.0167	10.4302	387.8940	9.9402	368.7485	9.4496
	III	260.5236	26.4819	260.5496	26.4652	206.5784	26.4689
	IV	0	40.9340	0	40.9337	0	40.9334
$(0/P/90/0/90)_S$	I	406.8270	0	387.5548	0	368.2604	0
	II	395.5050	5.0676	376.3122	4.8217	357.0951	4.5755
	III	183.0540	23.4536	183.0664	23.4563	183.0904	23.4594
	IV	0	35.5569	0	35.5566	0	35.5564
$(P/(0/90)_4/P)_T$	I	428.2886	0	408.9482	0	389.6208	0
	II	415.0231	10.6354	395.9119	10.1456	376.7783	9.6553
	III	232.3520	29.7713	232.3841	29.7754	232.4193	29.7799
	IV	0	47.1077	0	47.1073	0	47.1070
$(0/P/(90/0)_3/P/90)_T$	I	412.6404	0	393.3018	0	373.9675	0
	II	400.0673	10.6079	380.8411	9.7594	361.6068	9.2665
	III	229.7813	29.4419	229.8132	29.4460	229.8482	29.4504
	IV	0	46.5861	0	46.5857	0	46.5854
$\overline{Z} = 500$							
$(P/(0/90)_2)_S$	I	429.3031	0	409.9954	0	390.6703	0
	II	419.1593	5.3707	399.9236	5.1242	380.4678	4.8775
	III	154.8400	19.8397	154.8440	19.8402	154.8486	19.8408
	IV	0	26.14704	0	26.14698	0	26.14695
$(0/P/90/0/90)_S$	I	408.6986	0	389.3907	0	370.0630	0
	II	395.5372	5.0680	376.4170	4.8230	357.2700	4.5777
	III	136.2763	17.4611	136.2796	17.4615	136.2833	17.4620
	IV	0	22.71970	0	22.71965	0	22.71962
$(P/(0/90)_4/P)_T$	I	429.1577	0	409.8042	0	390.4507	0
	II	415.0191	10.6353	395.8705	10.1446	376.7004	9.6557
	III	177.2671	22.7132	177.2722	22.7139	177.2779	22.7146
	IV	0	30.37182	0	30.37175	0	30.37170
$(0/P/(90/0)_3/P/90)_T$	I	413.7106	0	394.3670	0	375.0172	0
	II	399.8684	10.2470	380.6515	9.7546	361.4200	9.2618
	III	176.5277	22.6185	176.5328	22.6192	176.5385	22.6199
	IV	0	30.24882	0	30.24874	0	30.24869

[a] I: pure thermal loading ($b_2 = 0$), II: combined loading case (2) ($b_2 = 0.01$ or 0.02), III: combined loading case (1) ($b_1 = 10$), IV: pure lateral pressure ($b_1 = 0$).

electric loading cases. It can be seen that the minus control voltages $V_U = V_L = -100$ V make the shell panel contract so that the buckling temperature is increased and the postbuckled deflection is decreased at the same temperature rise. In contrast, the plus control voltages $V_U = V_L = +100$ V decrease the buckling temperature and induce more large postbuckled deflections. The buckling temperature and postbuckling thermal loads are decreased by increasing the load-proportional parameter b_2. It can also be seen that only a very weak "snap-through" phenomenon occurs in the postbuckling range and the imperfection sensitivity can be predicted only for very small geometric imperfections.

Table 3
Imperfection sensitivity λ^* for imperfect piezolaminated cylindrical shells subjected to combined heating and lateral pressure and under three sets of electric loading cases ($R/t = 300$, $\overline{Z} = 200$)

Lay-up	$V_U = V_L =$	$\overline{W}^*/t = 0.0$	$\overline{W}^*/t = 0.2$	$\overline{W}^*/t = 0.3$	$\overline{W}^*/t = 0.4$	$\overline{W}^*/t = 0.5$
$b_2 = 0.0$						
$(P/(0/90)_2)_S$	−100 V	1.0	0.9399	0.9160	0.8960	0.8791
	0 V	1.0	0.9392	0.9142	0.8933	0.8757
	+100 V	1.0	0.9386	0.9123	0.8904	0.8719
$(0/P/90/0/90)_S$	−100 V	1.0	0.9368	0.9121	0.8914	0.8738
	0 V	1.0	0.9360	0.9100	0.8883	0.8698
	+100 V	1.0	0.9351	0.9078	0.8850	0.8655
$b_2 = 0.01$						
$(P/(0/90)_2)_S$	−100 V	1.0	0.9384	0.9148	0.8949	0.8778
	0 V	1.0	0.9375	0.9130	0.8919	0.8740
	+100 V	1.0	0.9364	0.9104	0.8885	0.8696
$(0/P/90/0/90)_S$	−100 V	1.0	0.9353	0.9108	0.8901	0.8723
	0 V	1.0	0.9340	0.9082	0.8865	0.8679
	+100 V	1.0	0.9325	0.9054	0.8825	0.8628

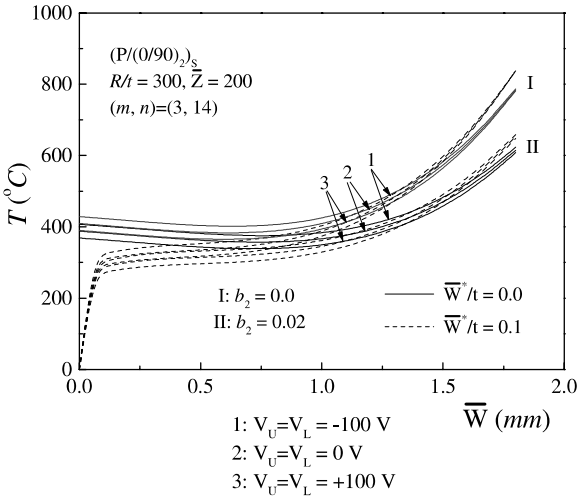

Fig. 2. Thermal postbuckling load–deflection curves of a $(P/(0/90)_2)_S$ cylindrical shell subjected to combined heating and lateral pressure and under electric loading cases.

Fig. 3 gives the thermal postbuckling load–deflection curves for a $(P/(0/90)_4/P)_T$ cylindrical shell under the same loading case of Fig. 1. Changes in buckling mode are clearly observed by increasing the load-proportional parameter b_2, i.e. $(m, n) = (4, 14)$ become $(m, n) = (3, 14)$, and the postbuckling load–deflection curves become sufficiently lower. It can also be seen that, under the loading case of heating alone ($b_2 = 0$), the thermal postbuckling behavior is stable and the shell structure becomes imperfection insensitive.

Fig. 4 compares the thermal postbuckling load–deflection curves for $(0/P/90/0/90)_S$ and $(0/P/(90/0)_3/P/90)_T$ cylindrical shells under combined loading case (2) with the load-proportional parameter $b_2 = 0.01$, and under three sets of electric loading cases. The results show that the thermal postbuckling load–deflection

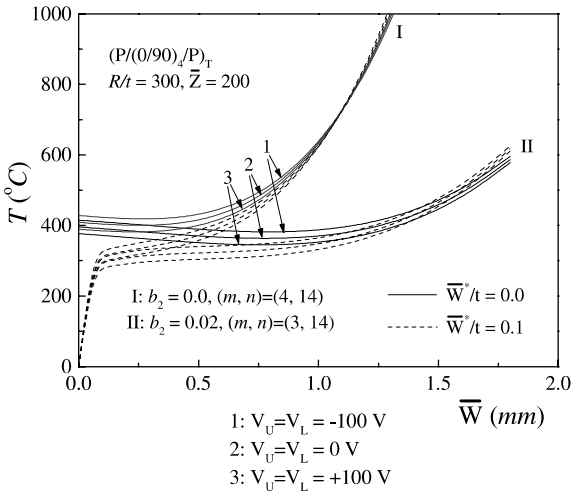

Fig. 3. Thermal postbuckling load–deflection curves of a $(P/(0/90)_4/P)_T$ cylindrical shell subjected to combined heating and lateral pressure and under electric loading cases.

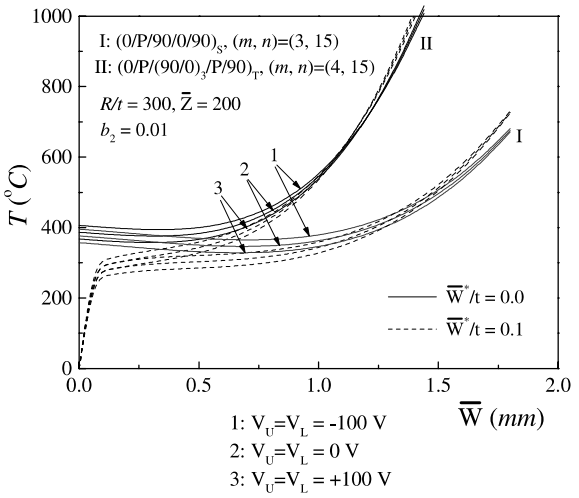

Fig. 4. Comparisons of thermal postbuckling load–deflection curves of $(0/P/90/0/90)_S$ and $(0/P/(90/0)_3/P/90)_T$ cylindrical shells subjected to combined heating and lateral pressure and under electric loading cases.

curves of $(0/90)_{2S}$ cylindrical shell is lower than that of $(0/90)_{4T}$ cylindrical shell with symmetrically embedded piezoelectric layers, when $\overline{W}/t > 0.5$.

Fig. 5 compares the thermal postbuckling load–deflection curves for $(P/(0/90)_4/P)_T$ and $(0/P/(90/0)_3/P/90)_T$ cylindrical shells under the same loading case of Fig. 3. The results show that the shell with embedded piezoelectric layers has lower buckling temperature, but has higher postbuckling strength when the deflection $\overline{W}$ is sufficiently large.

Fig. 6 shows the effect of shell geometric parameter $\overline{Z}$ (=200 and 500) on the thermal postbuckling behavior of $(P/(0/90)_2)_S$ cylindrical shells under combined loading case (2) with the load-proportional parameter $b_2 = 0.01$, and under three sets of electric loading cases. The results show that the buckling

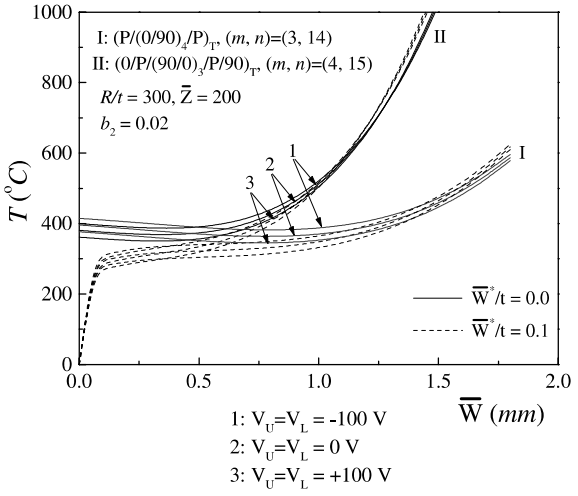

Fig. 5. Comparisons of thermal postbuckling load–deflection curves of $(P/(0/90)_4/P)_T$ and $(0/P/(90/0)_3/P/90)_T$ cylindrical shells subjected to combined heating and lateral pressure and under electric loading cases.

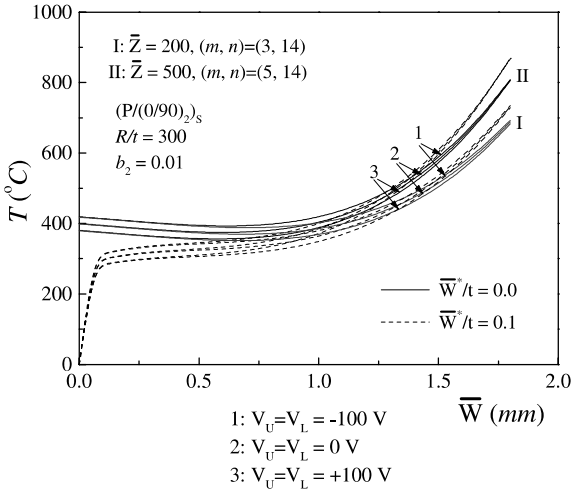

Fig. 6. Effect of shell geometric parameter on the thermal postbuckling load–deflection curves of $(P/(0/90)_2)_S$ cylindrical shells subjected to combined heating and lateral pressure and under electric loading cases.

temperatures compare very closely for these two shells. In contrast, the thermal postbuckling load–deflection curve of the shell with $\overline{Z} = 200$ is lower than that of the shell with $\overline{Z} = 500$, when $\overline{W}/t > 0.5$.

The effects of control voltages on the imperfection sensitivities of $(0/90)_{2S}$ laminated cylindrical shell with symmetrically fully covered or embedded piezoelectric layers under combined loading case (2) with the load-proportional parameter $b_2 = 0$ and 0.01 are shown in Table 3, and only a very small effect can be seen. In Table 3, λ^* is the maximum value of σ_x for the imperfect shell, made dimensionless by dividing by the critical value of σ_x for the perfect shell.

Figs. 7 and 8 show, respectively, the effects of control voltages on the postbuckling behavior of the same two cylindrical shells analogous to the cases of Figs. 2 and 3, but under combined loading case (1) with the

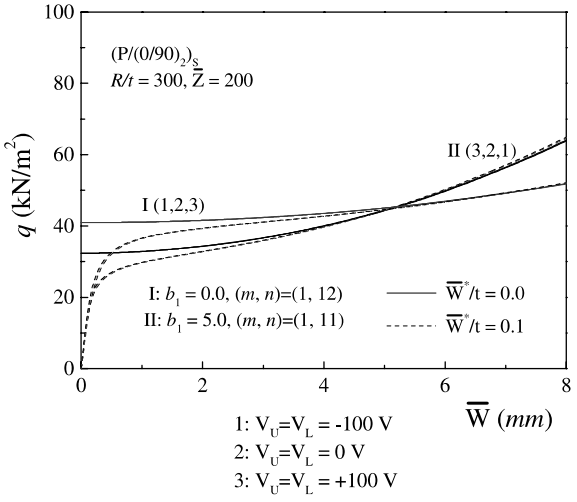

Fig. 7. Postbuckling load–deflection curves of a $(P/(0/90)_2)_S$ cylindrical shell subjected to combined lateral pressure and heating and under electric loading cases.

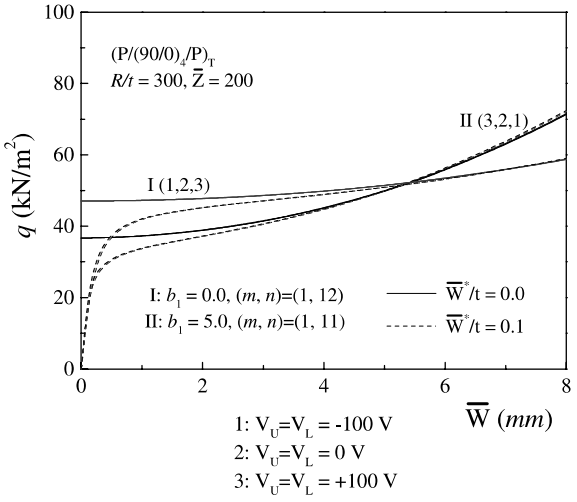

Fig. 8. Postbuckling load–deflection curves of a $(P/(0/90)_4/P)_T$ cylindrical shell subjected to combined lateral pressure and heating and under electric loading cases.

load-proportional parameter $b_1 = 0$ and 5.0. The results show that the curves 1, 2 and 3 are almost the same, and the control voltage has a very small effect on the postbuckling behavior. It can also be seen that an increase in pressure is usually required to obtain an increase in deformation, and the postbuckling path is stable for both perfect and imperfect shells, and the shell structure is virtually imperfection insensitive.

5. Concluding remarks

A postbuckling analysis has been presented for cross-ply laminated cylindrical shells with piezoelectric actuators subjected to combined action of external pressure and heating and under electric loading cases.

The temperature field considered is assumed to be a uniform distribution over the shell surface and through the shell thickness and the electric field is assumed to be the transverse component E_Z only. The material properties are assumed to be independent of the temperature and the electric field. The boundary layer theory of shell buckling has been extended to the case of hybrid cylindrical shells containing piezoelectric layers. A singular perturbation technique is employed to determine interactive buckling loads and post-buckling load–deflection curves. Extensive parametric studies for symmetric and antisymmetric cross-ply laminated shells with fully covered or embedded piezoelectric actuators have been carried out. The results presented herein show that the minus control voltages increase the buckling temperature and decrease the postbuckled deflection at the same temperature rise, whereas the plus control voltages decrease the buckling temperature and induce more large postbuckled deflections. They also show that the control voltage has a significant effect on the buckling loads under combined loading case (2). In contrast, it has a very small effect on the imperfection sensitivities of $(0/90)_{2S}$ laminated cylindrical shells with piezoelectric actuators. The results also confirm that the control voltage has a very small effect on the buckling loads under combined loading case (1), and the postbuckling behavior of piezolaminated cylindrical shells is stable and the shell structure is virtually imperfection insensitive.

Acknowledgements

This work is supported in part by the National Natural Science Foundation of China under Grant 59975058. The author is grateful for this financial support.

Appendix A

In Eqs. (27)–(28b)

$$\Theta_1 = \frac{1}{C_3}\left\{\frac{\gamma_{24}^2-\gamma_5^2}{\gamma_{24}}\frac{\gamma_{T1}-a_1\gamma_{T2}/2}{g_T}\lambda_q^{(2)} - \frac{\gamma_{T2}-\gamma_5\gamma_{T1}}{8g_T}\left[m^2\left(1+2\mu+\frac{1}{\pi\alpha}\varepsilon^{1/2}\right)-2g_3\varepsilon+\frac{g_3^2}{m^2}\varepsilon^2\right]\right\},$$

$$\Theta_2 = \varepsilon\frac{\gamma_{P2}-\gamma_5\gamma_{P1}}{\gamma_{24}}\Delta V - \frac{\gamma_{24}^2-\gamma_5^2}{\gamma_{24}}\frac{\gamma_{T1}-a_1\gamma_{T2}/2}{g_T}\lambda_q^{(0)},$$

$$\lambda_q^{(0)} = \left\{\frac{\gamma_{24}m^4}{(1+\mu)C_1g_2}+\frac{(2+\mu)}{(1+\mu)^2}\frac{m^2}{C_1}\frac{\gamma_{24}g_3}{g_2}\varepsilon+\frac{1}{(1+\mu)C_1}\left[\frac{g_1}{\gamma_{14}}+\frac{(1-\mu-\mu^2)}{(1+\mu)^2}\frac{\gamma_{24}g_3^2}{g_2}\right]\varepsilon^2\right.$$
$$\left.-\frac{\mu}{(1+\mu)^2}\frac{g_3}{m^2C_1}\left[1+\frac{g_3}{(1+\mu)m^2}\varepsilon\right]\left[\frac{g_1}{\gamma_{14}}+\frac{\gamma_{24}g_3^2}{g_2}\frac{(2+\mu)^2}{(1+\mu)^2}\right]\varepsilon^3\right\},$$

$$\lambda_q^{(2)} = \frac{1}{4}\left\{\frac{m^4n^2\beta^2}{g_2}\left[2\gamma_{24}(1+\mu)(2+\mu)+\frac{1}{4}\frac{(1+2\mu)g_2}{\gamma_{24}n^2\beta^2C_1}-\frac{\gamma_{24}n^2\beta^2g_2}{(1+\mu)C_1g_2-2a_1m^6}\right.\right.$$
$$\left.\left.\times\left(2(1+\mu)^2+\frac{1}{2}\frac{a_1m^2(1+2\mu)}{C_1}+(2+\mu)\frac{(1+2\mu)g_2+8m^4(1+\mu)}{g_2}\right)\right]\right\},$$

$$C_1 = n^2\beta^2+\frac{1}{2}a_1m^2 \tag{A.1}$$

and in Eqs. (32)–(33b)

$$C_{11}=\frac{g_8}{g_T},$$

$$\Theta_3=\frac{1}{C_3}\left\{\left(\frac{\gamma_{24}^2}{\gamma_{14}\gamma_{24}+\gamma_{34}^2}\right)\frac{m^4(1+\mu)}{16n^2\beta^2g_2}\varepsilon^{-1}+\frac{1}{32}\left(\frac{\gamma_{24}^2}{\gamma_{14}\gamma_{24}+\gamma_{34}^2}\right)\frac{m^2}{\gamma_{24}n^2\beta^2}\left[\frac{\gamma_{34}}{\gamma_{24}}(1+2\mu)-\frac{2\gamma_{24}g_3}{g_2}\right]\right.$$
$$\left.+\frac{\gamma_5}{8g_8}\left[m^2\left(1+2\mu+\frac{1}{\pi\alpha}\varepsilon^{1/2}\right)\varepsilon-2g_3\varepsilon^2+\frac{g_3^2}{m^2}\varepsilon^3\right]+\frac{\gamma_{24}^2-\gamma_5^2}{\gamma_{24}}\frac{\gamma_{T2}-a_2\gamma_{T1}}{g_T}\lambda_T^{(2)}\right\},$$

$$\Theta_4=\frac{\gamma_{24}^2-\gamma_5^2}{\gamma_{24}}\left[\frac{\gamma_{P2}-a_2\gamma_{P1}}{g_8}\Delta V+\frac{\gamma_{T2}-a_2\gamma_{T1}}{g_T}\lambda_T^{(0)}\right],$$

$$\lambda_T^{(0)}=C_2\left\{\frac{\gamma_{24}m^2}{(1+\mu)g_2}\varepsilon^{-1}+\gamma_{24}\frac{(2+\mu)g_3}{(1+\mu)^2g_2}+\frac{1}{(1+\mu)m^2}\left[\frac{g_1}{\gamma_{14}}+\gamma_{24}\frac{g_3^2}{g_2}\frac{(1-\mu-\mu^2)}{(1+\mu)^2}\right]\varepsilon\right.$$
$$\left.-\frac{\mu}{(1+\mu)^2}\frac{g_3}{m^4}\left[1+\frac{g_3}{(1+\mu)m^2}\varepsilon\right]\left[\frac{g_1}{\gamma_{14}}+\gamma_{24}\frac{g_3^2}{g_2}\frac{(2+\mu)^2}{(1+\mu)^2}\right]\varepsilon^2\right\},$$

$$\lambda_T^{(P)}=\frac{g_P}{g_8}\Delta V,$$

$$\lambda_T^{(2)}=\frac{1}{4}C_2\left\{\left(\frac{\gamma_{24}^2}{\gamma_{14}\gamma_{24}+\gamma_{34}^2}\right)\frac{\gamma_{24}m^6(2+\mu)}{2g_2^2}\varepsilon^{-1}\right.$$
$$+\left(\frac{\gamma_{24}^2}{\gamma_{14}\gamma_{24}+\gamma_{34}^2}\right)\frac{m^4}{2g_2}\left[\frac{\gamma_{34}}{\gamma_{24}}\frac{(1+\mu)^2+(1+2\mu)}{1+\mu}+\gamma_{24}\frac{g_3}{g_2}\frac{\mu(3+\mu)}{(1+\mu)}\right]-\frac{1}{4}\left(\frac{\gamma_{14}}{\gamma_{14}\gamma_{24}+\gamma_{34}^2}\right)m^2(1+2\mu)\varepsilon$$
$$+\varepsilon\frac{\gamma_{24}m^2n^4\beta^4}{g_2}\frac{g_2[(4+9\mu+4\mu^2)+C_2(1+2\mu)]+8m^4(1+\mu)(2+\mu)}{g_2(1+\mu)-4m^4C_2}$$
$$-\left(\frac{\gamma_{24}^2}{\gamma_{14}\gamma_{24}+\gamma_{34}^2}\right)\frac{m^2g_3}{4g_2}\left[\frac{\gamma_{34}}{\gamma_{24}}\frac{(4+12\mu+15\mu^2+4\mu^3)}{(1+\mu)^2}+2\gamma_{24}\frac{g_3}{g_2}\frac{(4+\mu+2\mu^2+\mu^3)}{(1+\mu)^2}\right]\varepsilon$$
$$\left.-\frac{\gamma_{24}}{2g_8}\left[m^2\left(1+2\mu+\frac{1}{\pi\alpha}\varepsilon^{1/2}\right)\varepsilon-2g_3\varepsilon^2+\frac{g_3^2}{m^2}\varepsilon^3\right]\right\},$$

$$\lambda_T^{(4)}=\frac{1}{64}C_2\left(\frac{\gamma_{24}^2}{\gamma_{14}\gamma_{24}+\gamma_{34}^2}\right)^2\frac{\gamma_{24}m^{10}(1+\mu)}{g_2^3}\varepsilon^{-1}$$
$$\times\frac{g_{13}[C_9(1+3\mu+\mu^2)+C_5(4+2\mu)+(1+\mu)]+g_2[C_5(6+8\mu+2\mu^2)-(2\mu+3\mu^2+\mu^3)]}{g_{13}C_9-g_2(1+\mu)}$$
$$+\frac{1}{64}C_2\frac{\gamma_{24}}{g_8}\left\{\frac{b}{32\pi\alpha}\left(\frac{\gamma_{24}^2}{\gamma_{14}\gamma_{24}+\gamma_{34}^2}\right)^2\frac{m^8(1+\mu)^2}{n^4\beta^4g_2^2}\varepsilon^{-3/2}\right.$$
$$\left.+m^2n^4\beta^4(1+\mu)^2\varepsilon^3\left[\frac{g_2(1+2\mu)+8m^4(1+\mu)}{g_2(1+\mu)-4m^4C_2}\right]^2\right\},$$

$$C_2=\frac{m^2}{m^2+a_2n^2\beta^2},\quad C_5=\frac{m^2+5a_2n^2\beta^2}{m^2+a_2n^2\beta^2},\quad C_9=\frac{m^2+9a_2n^2\beta^2}{m^2+a_2n^2\beta^2}$$

in the above equations

$$
\begin{aligned}
&g_1 = m^4 + 2\gamma_{12}m^2n^2\beta^2 + \gamma_{14}^2 n^4\beta^4, \quad g_2 = m^4 + 2\gamma_{22}m^2n^2\beta^2 + \gamma_{24}^2 n^4\beta^4,\\
&g_3 = \gamma_{30}m^4 + \gamma_{32}m^2n^2\beta^2 + \gamma_{34}n^4\beta^4, \quad g_{13} = m^4 + 18\gamma_{22}m^2n^2\beta^2 + 81\gamma_{24}^2 n^4\beta^4,\\
&C_3 = 1 - \frac{g_3}{m^2}\varepsilon, \quad b = \left(\frac{\gamma_{14}\gamma_{24}}{1+\gamma_{14}\gamma_{24}\gamma_{30}^2}\right)^{1/2}, \quad c = -\frac{\gamma_{14}\gamma_{24}\gamma_{30}}{1+\gamma_{14}\gamma_{24}\gamma_{30}^2}, \quad \alpha = \left[\frac{b-c}{2}\right]^{1/2}, \quad \phi = \left[\frac{b+c}{2}\right]^{1/2},\\
&g_8 = \gamma_{24}^2 - a_2\gamma_5 - \frac{4}{\pi}\frac{\alpha}{b}\gamma_5(\gamma_5 - a_2)\varepsilon^{1/2},\\
&g_T = (\gamma_{24}^2\gamma_{T1} - \gamma_5\gamma_{T2}) + \frac{4}{\pi}\frac{\alpha}{b}\gamma_5(\gamma_{T2} - \gamma_5\gamma_{T1})\varepsilon^{1/2},\\
&g_P = (\gamma_{24}^2\gamma_{P1} - \gamma_5\gamma_{P2}) + \frac{4}{\pi}\frac{\alpha}{b}\gamma_5(\gamma_{P2} - \gamma_5\gamma_{P1})\varepsilon^{1/2}.
\end{aligned}
\tag{A.3}
$$

References

Balamurugan, V., Narayanan, S., 2001. Active vibration control of smart shells using distributed piezoelectric sensors and actuators. Smart Materials and Structures 10, 173–180.

Batdorf, S.B., 1947. A simplified method of elastic-stability analysis for thin cylindrical shells. NACA TR-874.

Birman, V., Simonyan, A., 1994. Theory and applications of cylindrical sandwich shells with piezoelectric sensors and actuators. Smart Materials and Structures 3, 391–396.

Chen, C.Q., Shen, Y.P., Wang, X.M., 1996. Exact solution of orthotropic cylindrical shell with piezoelectric layers under cylindrical bending. International Journal of Solids and Structures 33, 4481–4494.

Correia, I.F., Soares, C.M., Soares, C.A., Herskovits, J., 1999. Development of semianalytical axisymmetric shell models with embedded sensors and actuators. Composite Structures 47, 531–541.

Kapuria, S., Sengupta, S., Dumir, P.C., 1997. Three-dimensional solution for a hybrid cylindrical shell under axisymmetric thermoelectric load. Archive of Applied Mechanics 67, 320–330.

Koconis, D.B., Kollar, L.P., Springer, G.S., 1994. Shape control of composite plates and shells with embedded actuators: I Voltages specified. Journal of Composite Materials 28, 415–458.

Lee, H.J., Saravanos, D.A., 2000. Mixed multi-field finite element formulation for thermopiezoelectric composite shells. International Journal of Solids and Structures 37, 4949–4967.

Li, Q.S., Liu, D.K., Zhang, N., Tam, C.M., Yang, L.F., 2001. Multilevel design and genetic algorithm for structural control system optimization. Earthquake Engineering and Structural Dynamics 30, 927–942.

Oh, I.K., Han, J.H., Lee, I., 2000. Postbuckling and vibration characteristics of piezolaminated composite plate subjected to thermo-piezoelectric loads. Journal of Sound and Vibration 233, 19–40.

Reddy, J.N., 1999. On laminated composite plates with integrated sensors and actuators. Engineering Structures 21, 568–593.

Saravanos, D.A., 1997. Mixed laminate theory and finite element for smart piezoelectric composite shell structures. AIAA Journal 35, 1327–1333.

Shen, H.S., Chen, T.Y., 1988. A boundary layer theory for the buckling of thin cylindrical shells under external pressure. Applied Mathematics and Mechanics 9, 557–571.

Shen, H.S., Chen, T.Y., 1990. A boundary layer theory for the buckling of thin cylindrical shells under axial compression. In: Chien, W.Z., Fu, Z.Z. (Eds.), Advances in Applied Mathematics and Mechanics in China, vol. 2. International Academic Publishers, Beijing, China, pp. 155–172.

Shen, H.S., Chen, T.Y., 1991. Buckling and postbuckling of cylindrical shells under combined external pressure and axial compression. Thin-Walled Structures 12, 321–334.

Shen, H.S., Zhou, P., Chen, T.Y., 1993. Postbuckling analysis of stiffened cylindrical shells under combined external pressure and axial compression. Thin-Walled Structures 15, 43–63.

Shen, H.S., 1997a. Post-buckling analysis of imperfect stiffened laminated cylindrical shells under combined external pressure and axial compression. Computers and Structures 63, 335–348.

Shen, H.S., 1997b. Thermal postbuckling analysis of imperfect stiffened laminated cylindrical shells. International Journal of Non-Linear Mechanics 32, 259–275.

Shen, H.S., 1997c. Thermomechanical postbuckling analysis of stiffened laminated cylindrical shell. ASCE Journal of Engineering Mechanics 123, 433–443.

Shen, H.S., 1998a. Postbuckling analysis of stiffened laminated cylindrical shells under combined external liquid pressure and axial compression. Engineering Structures 20, 738–751.

Shen, H.S., 1998b. Postbuckling analysis of imperfect stiffened laminated cylindrical shells under combined external pressure and thermal loading. International Journal of Mechanical Sciences 40, 339–355.

Shen, H.S., 1999. Thermomechanical postbuckling of composite laminated cylindrical shells with local geometric imperfections. International Journal of Solids and Structures 36, 597–617.

Shen, H.S., 2001. Postbuckling of shear deformable laminated plates with piezoelectric actuators under complex loading conditions. International Journal of Solids and Structures 38, 5377–5390.

Tani, J., Qiu, J., Miura, H., 1995. Vibration control of a cylindrical shell using piezoelectric actuators. Journal of Intelligent Material Systems and Structures 6, 380–388.

Tsai, S.W., Hahn, H.T., 1980. Introduction to Composite Materials. Technomic Publishing Co., Westport, CT.

Tzou, H.S., Gadre, M., 1989. Theoretical analysis of a multi-layered thin shell coupled with piezoelectric shell actuators for distributed vibration controls. Journal of Sound and Vibration 132, 433–450.